Flexible OLED

International Edition: DOI: 10.1002/anie.201600414
German Edition: DOI: 10.1002/ange.201600414

Versatile p-Type Chemical Doping to Achieve Ideal Flexible Graphene Electrodes

*Tae-Hee Han[+], Sung-Joo Kwon[+], Nannan Li, Hong-Kyu Seo, Wentao Xu, Kwang S. Kim, and Tae-Woo Lee**

Abstract: *We report effective solution-processed chemical p-type doping of graphene using trifluoromethanesulfonic acid (CF_3SO_3H, TFMS), that can provide essential requirements to approach an ideal flexible graphene anode for practical applications: i) high optical transmittance, ii) low sheet resistance (70 % decrease), iii) high work function (0.83 eV increase), iv) smooth surface, and iv) air-stability at the same time. The TFMS-doped graphene formed nearly ohmic contact with a conventional organic hole transporting layer, and a green phosphorescent organic light-emitting diode with the TFMS-doped graphene anode showed lower operating voltage, and higher device efficiencies (104.1 cd A^{-1}, 80.7 lm W^{-1}) than those with conventional ITO (84.8 cd A^{-1}, 73.8 lm W^{-1}).*

The widely used indium tin oxide (ITO) transparent electrode is not appropriate for use in flexible electronics, because it is brittle, increasingly expensive, and causes diffusion of impurities into devices.[1–3] Therefore, flexible transparent electrodes must be developed before the use of flexible electronics is practical. Graphene is a one atom thick sheet of sp^2 hybridized carbon atoms that has unique electrical properties and mechanical robustness.[2,4–11] Therefore, many researchers have explored ways to use graphene electrodes in flexible organic optoelectronics.[2,12–22] However, the pristine graphene has suffered from two inherent major problems: 1) The first disadvantage comes from its low charge carrier density. Therefore, the pristine graphene has much higher sheet resistance (200–300 $\Omega\,sq^{-1}$) than does ITO ($\approx 10\ \Omega\,sq^{-1}$), which resulted in high operating voltage and poor luminous power efficiency (*PE*) in organic light-emitting diodes (OLEDs),[15,16] and thus graphene requires an additional doping process to improve the charge carrier concentration and the electrical conductivity.[2,20–27] 2) The pristine graphene's work function ($WF = 4.4$ eV) is much lower than that of ITO (4.8 eV).[2] The low *WF* of the pristine graphene significantly limits the hole injection from the graphene anode to an overlying organic layers in OLEDs.[2,15,16] The nitric acid (HNO_3) and the gold (III) chloride ($AuCl_3$) have been widely used as chemical p-type dopants for graphene to reduce sheet resistance (R_s).[2,6,21–23] However, these conventional chemical dopants cause instability problems: the HNO_3 gradually evaporates from the graphene in the ambient condition due to its volatility, thereby causing gradual decrease of electrical conductivity of the p-doped graphene and its device;[2a,22–24] The $AuCl_3$ leaves 50–100 nm Au particles on the graphene surface, which degrades device efficiency and stability increasing current leakage in the thin film devices.[2a] Therefore, to fabricate ideal graphene anodes for organic optoelectronics needs a versatile p-type doping method that can meet essential requirements at the same time: i) high optical transmittance (*OT*), ii) the low R_s comparable to that of ITO, iii) the high surface *WF* that can effectively reduce the hole injection energy barrier, iv) a smooth surface after chemical doping, and v) air-stability that maintains doping effect in the ambient condition. When p-type doping can sufficiently reduce the R_s and greatly increase the surface *WF* of the graphene anode at the same time, it can facilitate hole injection from the graphene anode to the conventional vacuum-deposited hole injection or transporting layers (HILs or HTLs) without specially developed HILs.[2a]

Here, we report versatile solution-processed chemical p-type doping of graphene using a novel dopant, trifluoromethanesulfonic acid (CF_3SO_3H, TFMS) (Figure 1 a). The TFMS is one of the strongest monoprotonic organic acid; TFMS also has outstanding thermal and chemical stability.[28–30] Simple spin-coating of TFMS dissolved in a nitromethane effectively p-doped the graphene resulting in great decrease of R_s and large increase of surface *WF* of the graphene with an excellent air-stability. We synthesized large-area single-layer graphene (SLG) by chemical vapor deposition (CVD) (Table S1 in the Supporting Information). To form four-layered graphenes (4LGs), SLGs were repeatedly transferred and stacked onto a substrate. The pristine 4LG has $OT > 90\,\%$ at 550 nm; therefore the transfer and stacking process did not significantly disrupt the optical properties of the graphene (Figure S1). Although p-type chemical doping slightly decreased *OT* due to increased charge carrier density,[31] the p-doped 4LG maintained sufficiently high *OT* with HNO_3 (87.3 %) and TFMS (88.3 %) as a transparent electrode in OLEDs. The chemically p-doped graphene had a smooth surface without large particle formation (Figure S2).

Raman spectroscopy was used to determine the p-type doping effects of chemical dopants. The intensity ratio of 2D band ($I_{2D} = 2679\ cm^{-1}$) to G band ($I_G = 1592\ cm^{-1}$) of SLG was 1.44 and the D band intensity (I_D) was negligible

[*] Dr. T.-H. Han,[+] S.-J. Kwon,[+] H.-K. Seo, Dr. W. Xu, Prof. T.-W. Lee
Department of Materials Science and Engineering
Pohang University of Science and Technology (POSTECH)
San 31, Hyoja-dong, Nam-gu, Pohang, Gyungbuk 790-784 (Republic of Korea)
E-mail: twlee@postech.ac.kr
Dr. N. Li, Prof. K. S. Kim
Department of Chemistry
Ulsan National Institute of Science and Technology (UNIST)
Ulsan, 689-798 (Republic of Korea)
[+] These authors contributed equally to this work.

Supporting information for this article can be found under: http://dx.doi.org/10.1002/anie.201600414.

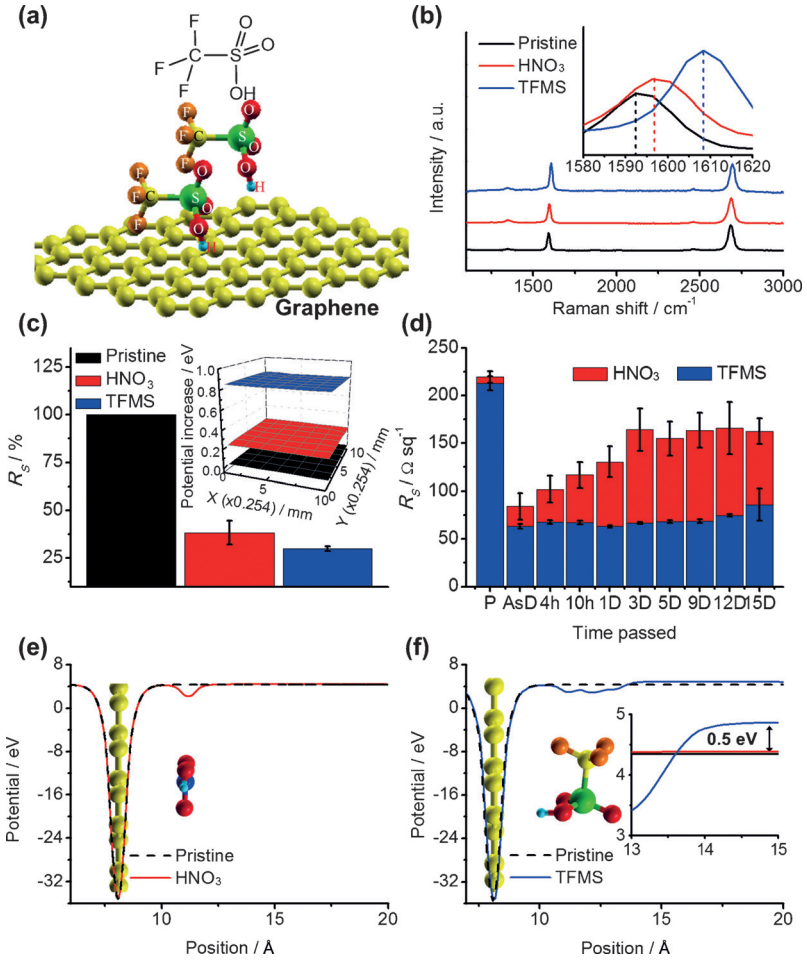

Figure 1. a) Chemical structure of trifluoromethanesulfonic acid (TFMS) (top) and schematic illustration of TFMS-doped graphene (bottom). b) Raman spectra of the pristine and p-doped single-layer graphenes (inset: G band shift). c) Relative sheet resistance (inset: surface potential increase) of the pristine and p-type doped 4LGs. d) Sheet resistance change with time of HNO_3- and TFMS-doped 4LG under ambient conditions. e,f) Planar average of electrostatic potential and the most stable adsorption configuration of HNO_3- (e) and TFMS-doped (f) graphene and pristine graphene. The Fermi level is shifted to zero (inset: difference in work function between HNO_3- and TFMS-doped graphene).

compared to other characteristic peaks ($I_D/I_G < 0.1$) (Figure 1b). This result proves high-quality SLG growth and successful transfer without significant structural defects. The p-type doping of the graphene upshifted the 2D and G bands of Raman spectroscopy due to phonon stiffening effect;[32–34] the TFMS-doped SLG exhibited more upshifted 2D band at 2695 cm^{-1} and the G band at 1610 cm^{-1} than those with HNO_3 (2D: 2685 cm^{-1}, G: 1596 cm^{-1}). p-Type doping of graphene also decreases I_{2D}/I_G and the full-width-half-maximum (FWHM) of the G band;[33,34] the TFMS doping of SLG also caused larger decreases in intensity ratio of 2D to G band ($I_{2D}/I_G = 0.97$) and FWHM (19.9 cm^{-1}) than did HNO_3 doping ($I_{2D}/I_G = 1.3$; FWHM 22.1 cm^{-1}) (Figure S3). Neither dopant made change in the D band; this result means that solution-processed doping does not cause significant structural defects in the graphene. Results of Raman spectroscopy demonstrate that the TFMS has strong p-doping ability for the graphene.

The TFMS effectively reduced R_s of 4LG by 70% (Pristine: $212.7 \pm 7.2\ \Omega\,sq^{-1}$, TFMS-doped: $63.3 \pm 2.5\ \Omega\,sq^{-1}$) (Figure 1c). The TFMS doping also produced a uniform and significant surface potential increase of the 4LG by 830 meV in large-area Kelvin probe measurement ($> 1.5 \times 1.5\ mm^2$) (Figure 1c inset). Therefore, the estimated surface *WF* of the TFMS-doped 4LG is 5.23 eV. Conventional HNO_3 doping also decreased R_s of the pristine graphene by 62% ($84.0 \pm 13.8\ \Omega\,sq^{-1}$) that coincides with previous report,[6] but did not significantly increase the surface potential of the 4LG (210 meV). Furthermore, in ambient condition, the R_s of the HNO_3-doped 4LG gradually increased over time by > 70% of the pristine 4LG within 3 days, and then saturated (Figure 1d). In contrast, TFMS-doped 4LG maintained reduced R_s and showed no significant change for 15 days in ambient condition (Figure 1d).

To confirm our experimental observations according to graphene dopants, we performed a theoretical study by using a first-principles method (Supporting Information). First of all, we carried out the binding energy calculation to determine the most stable adsorption position for dopants on the graphene. The most energetically favorable adsorption position for each systems is shown in Figure 1e and f (Figures S4–S6). The TFMS molecule has higher binding energy (−0.50 eV) with the graphene than that of the HNO_3 molecule (−0.33 eV), which indicates stronger interaction between TFMS and graphene than that with the HNO_3. Furthermore, we confirmed this point by performing the charge transfer calculation, which shows that the electrons transferred from graphene to the TFMS molecule (0.052e per molecule) was about three times higher than that to HNO_3 molecule (0.018e per molecule). Here, we need to mention that the calculated charge transfer amount is quite small because the theoretical calculation system is a closed system. However, the charge transfer can be substantially enhanced and show an evident p-type doping effect in experimental environment (i.e., open system). Secondly, we investigated the *WF* of the HNO_3- and TFMS-doped graphene (Figure 1e,f). Although both p-dopings increased the *WF* of the pristine graphene (calculated *WF* of the pristine graphene 4.35 eV), the *WF* of the TFMS doped graphene was 0.5 eV higher than that with the HNO_3, which is qualitatively consistent with experimental observation by using Kelvin probe (0.6 eV) (Figure 1f inset).

Acidic proton binds to the graphene and immobilizes equivalent amount of electrons causing p-type doping of the graphene. The much stronger p-type doping effect of the TFMS demonstrated by experimental results and theoretical calculations could originate from more tightly and closely

bound acidic proton to the graphene; this would be attributed to the non-planar configuration (Figure 1 f), and stronger acidity of the TFMS than those with HNO_3.[28–30] As a result, hole carrier density of the TFMS-doped graphene increased, and thus it exhibited significantly increased electrical conductivity and shifted Fermi energy level. In addition, high ionization potential of trifluoromethane in TFMS could result in additional increase of graphene's surface *WF* in the Kelvin probe measurement. Because the protons in the HNO_3 are more directly exposed to the air due to its planar configuration on graphene than those of the TFMS, the superior air-stability of the TFMS-doped graphene compared with HNO_3 can also be attributed to non-planar configuration, higher binding energy, more hydrophobic nature of TFMS including trifluoromethane, and excellent chemical stability of the TFMS.[28–31]

We performed dark-injection space-charge-limited current (DI-SCLC) transient measurement to investigate hole injection properties of the TFMS-doped 4LG anode. We also calculated the hole injection efficiency (η) in hole-only devices (HODs) using the pristine and p-doped 4LG anodes. We employed widely-used hole transporting layer (HTL), *N,N′*-Di(1-naphthyl)-*N,N′*-diphenyl-(1,1′-biphenyl)-4,4′-diamine (NPB), on top of the graphene anode [4LG/ NPB (2 μm)/Al]. Because the NPB has a highest occupied molecular orbital (HOMO) energy level of 5.4 eV, pristine 4LG's low *WF* (4.4 eV) causes a large energy barrier for hole injection (1.0 eV); this large barrier significantly degrades η. Therefore, HOD with the pristine graphene anode showed extremely low current (Figure 2 a). In contrast, HODs with p-doped graphene anode showed a typical transient current shape; it indicates that ohmic contact was formed on the graphene anode (Figure 2 a). The TFMS-doped 4LG had higher hole current density in DI-SCLC due to its higher surface *WF* (5.23 eV) than those with HNO_3 (*WF* = 4.61 eV). Hole injection can more easily overcome the small hole injection energy barrier (0.17 eV) between the TFMS-doped 4LG and the HTL. We calculated η by using theoretical SCLC (Supporting information).[2a] The η was higher with the TFMS-doped 4LG than that with the HNO_3; the η with the TFMS-doped 4LG anode was 0.84, which means that simple solution-processing of TFMS on the graphene can achieve nearly ohmic contact for the hole injection to a conventional HTL without particular HILs.

We also fabricated green phosphorescent OLEDs with the pristine or the TFMS-doped 4LG, and with ITO anode. We employed a widely used small-molecule HIL, *N,N′*-diphenyl-*N,N′*-bis-[4-(phenyl-*m*-tolyl-amino)-phenyl]-biphenyl-4,4′-diamine (DNTPD), that has HOMO of 5.1–5.2 eV (Figure 2 c).[35] Green phosphorescent OLEDs with the ITO anode showed a large difference of device performances dependent on a surface treatment of ultra-violet ozone (UVO). The OLED on the untreated ITO showed much inferior current density and luminance characteristics than those with UVO surface-treated ITO (UVO-ITO) (Figure 2 d,e). Because UVO increases surface *WF* of ITO by > 0.3 eV,[36] the device with untreated ITO has a larger energy barrier for hole injection than does the device with UVO-ITO; the *WF* difference between anodes significantly changed operating voltage of OLEDs (Figure 2 e).

The OLED with the pristine 4LG anode exhibited much lower current density and luminance characteristics even than those with the untreated ITO anode (Figure 2 d,e). The lower surface *WF* (4.4 eV) and higher R_s ($> 200\ \Omega\,sq^{-1}$) of the pristine 4LG than those with the untreated ITO significantly degraded hole injection and increased operating voltage of OLEDs. Therefore, simple replacement of the ITO anode with the pristine graphene anode in conventionally structured OLEDs degrades their current and luminance. However,

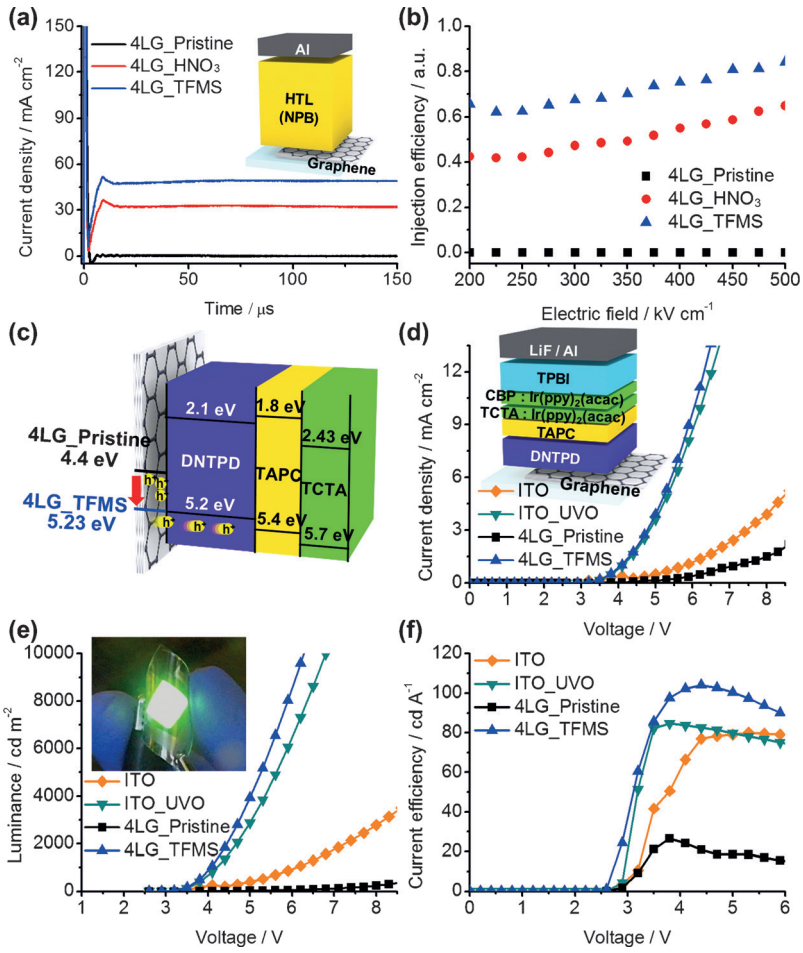

Figure 2. a) Transient current density of dark-injection space-charge-limited current measured at a 50 V. b) Hole injection efficiency versus electric field of hole-only devices using the pristine and p-type doped 4LG anodes. c) Schematic illustration of energy band diagram. d) Current density (inset: OLED structure). e) Luminance (inset: optical image flexible OLED with TFMS-doped 4LG anode (light emitting area: 1 cm × 1 cm) on the PET substrate). f) Current efficiency of OLEDs with untreated ITO, UVO-ITO, pristine 4LG anode and TFMS-doped 4LG anode.

TFMS doping of the graphene greatly improved its hole injection by increasing its surface *WF*, and decreased the operating voltage by synergy of increased hole injection and decreased R_s of the graphene anode (Figure 2c). The OLED with the TFMS-doped 4LG anode exhibited significantly increased current density and luminance which were even higher than those with the conventionally used UVO-ITO anode (Figure 2d,e). Even though the TFMS-doped graphene has higher R_s (63 $\Omega\,sq^{-1}$) than does ITO (10 $\Omega\,sq^{-1}$), the high surface *WF* of the TFMS-doped 4LG (5.23 eV) effectively contributes to reducing the operating voltage (TFMS-doped 4LG: 6.3 V and ITO-UVO: 6.8 V to emit 10000 $cd\,m^{-2}$) (Figure 2e). Improved η also directly affected the luminous current efficiency (*CE*) and *PE* of OLEDs. Devices with the pristine 4LG anode that has poor η showed the lowest *CE* (26.5 $cd\,A^{-1}$) and *PE* (21.9 $lm\,W^{-1}$) among the OLEDs fabricated in this work (Figure 2f, S7). Similarly, the device with the untreated ITO that has lower surface *WF* and poorer hole injection showed lower *CE* (80.1 $cd\,A^{-1}$) and *PE* (55.0 $lm\,W^{-1}$) than that with the UVO-ITO (84.8 $cd\,A^{-1}$ and 73.8 $lm\,W^{-1}$). The OLEDs with the TFMS-doped 4LG had higher *CE* (104.1 $cd\,A^{-1}$) and *PE* (80.7 $lm\,W^{-1}$) than did device with the UVO-ITO (Figure 2f, S7). More energetically favorable hole injection from the TFMS-doped 4LG anode could improve the balance of charge carrier injection and transport to the emitting layer in the OLED.[2a] Simple solution-processed doping of the pristine graphene anode greatly improved the performance of OLEDs: devices with TFMS-doped graphene anode had lower turn-on and operating voltages, and much higher *CE* and *PE* than did devices with the conventional ITO anode at the same time.

We additionally fabricated flexible OLED using TFMS-doped 4LG that has large emitting area (1 cm × 1 cm) on the polyethylene terephthalate substrate to demonstrate scalability and flexibility of our device based on TFMS-doped 4LG anode for practical applications. The OLEDs with TFMS-doped 4LG showed stable operation during flexion (Figure 2e inset), and a number of bending of device did not cause any defects in light emitting of OLEDs (Supporting video S1).

In conclusion, we developed a simple solution-processed chemical p-doping method of flexible transparent graphene electrodes to decrease R_s (70% decrease), increase *WF* (0.83 eV increase), and improve air-stability at the same time, and then achieved low operating voltage and high-efficiency in green phosphorescent OLEDs (104.1 $cd\,A^{-1}$, 80.7 $lm\,W^{-1}$) with the TFMS-doped 4LG anode. The strong p-type doping effect and air-stability of the TFMS on the graphene can be attributed to strong acidic nature and non-planar molecular configuration of TFMS resulting in tightly and closely bound acidic proton to the graphene. This kind of versatile p-type doping of graphene to increase its electrical conductivity, surface *WF*, and air-stability provides a method to achieve OLEDs that are superior to conventional rigid OLEDs with the ITO anode, and does not require a special HIL to compensate for graphene's low electrical conductivity and low *WF*.

Acknowledgements

This work was supported by a National Research Foundation of Korea (NRF) grant funded by the Korea government (MSIP) (NRF-2013R1A2A2A01068753), the Ministry of Science, ICT and Future Planning (MSIP), Korea, under the "IT Consilience Creative Program" (IITP-2015-R0346-15-1007).

Keywords: chemical doping · flexible OLEDs · graphene · transparent electrodes

How to cite: *Angew. Chem. Int. Ed.* **2016**, *55*, 6197–6201
Angew. Chem. **2016**, *128*, 6305–6309

[1] A. Kumar, C. Zhou, *ACS Nano* **2010**, *4*, 11.
[2] a) T.-H. Han, Y. Lee, M.-R. Choi, S.-H. Woo, S.-H. Bae, B. H. Hong, J.-H. Ahn, T.-W. Lee, *Nat. Photonics* **2012**, *6*, 105; b) T.-H. Han, S.-H. Jeong, Y. Lee, H.-K. Seo, S.-J. Kwon, M.-H. Park, T.-W. Lee, *J. Inf. Disp.* **2015**, *16*, 71; c) M.-H. Park, T.-H. Han, Y.-H. Kim, S.-H. Jeong, Y. Lee, H. Cho, T.-W. Lee, *J. Photonics Energy* **2015**, *5*, 053599; d) H. Cho et al., *2D Mater.* **2015**, *2*, 014002; e) T.-H. Han, S.-J. Kwon, H.-K. Seo, T.-W. Lee, *2D Mater.* **2016**, *3*, 014003; f) W. Xu, T.-S. Lim, H.-K. Seo, S.-Y. Min, H. Cho, M.-H. Park, Y.-H. Kim, T.-W. Lee, *Small* **2014**, *10*, 1999; g) W. Xu, H.-K. Seo, S.-Y. Min, H. Cho, T.-S. Lim, C.-Y. Oh, Y. Lee, T.-W. Lee, *Adv. Mater.* **2014**, *26*, 3459; h) W. Xu, L. Wang, Y. Liu, S. Thomas, H.-K. Seo, K.-I. Kim, K. S. Kim, T.-W. Lee, *Adv. Mater.* **2015**, *27*, 1619.
[3] A. Sharma, G. Andersson, D. A. Lewis, *Phys. Chem. Chem. Phys.* **2011**, *13*, 4381.
[4] K. S. Novoselov, A. K. Geim, S. V. Morozov, D. Jiang, Y. Zhang, S. V. Dubonos, I. V. Grigorieva, A. A. Firsov, *Science* **2004**, *306*, 666.
[5] K. S. Kim, Y. Zhao, H. Jang, S. Y. Lee, J. M. Kim, K. S. Kim, J.-H. Ahn, P. Kim, J.-Y. Choi, B. H. Hong, *Nature* **2009**, *457*, 706.
[6] S. Bae, H. Kim, Y. Lee, X. Xu, J.-S. Park, Y. Zheng, J. Balakrishnan, T. Lei, H. R. Kim, Y. I. Song, Y.-J. Kim, K. S. Kim, B. Özyilmaz, J.-H. Ahn, B. H. Hong, S. Iijima, *Nat. Nanotechnol.* **2010**, *5*, 574.
[7] Z. Sun, Z. Yan, J. Yao, E. Beitler, Y. Zhu, J. M. Tour, *Nature* **2010**, *468*, 549.
[8] F. Bonaccorso, Z. Sun, T. Hasan, A. C. Ferrari, *Nat. Photonics* **2010**, *4*, 611.
[9] C. N. R. Rao, A. K. Sood, K. S. Subrahmanyam, A. Govindaraj, *Angew. Chem. Int. Ed.* **2009**, *48*, 7752; *Angew. Chem.* **2009**, *121*, 7890.
[10] D. Ghosh, S. O. Kim, *Electron. Mater. Lett.* **2015**, *5*, 719.
[11] R. Narayan, S. O. Kim, *Nano Convergence* **2015**, *2*, 20.
[12] X. Wang, L. Zhi, N. Tsao, Z. Tomovic, J. Li, K. Mullen, *Angew. Chem. Int. Ed.* **2008**, *47*, 32990; *Angew. Chem.* **2008**, *120*, 3032.
[13] Y. Xue, J. Liu, H. Chen, R. Wang, D. Li, J. Qu, L. Dai, *Angew. Chem. Int. Ed.* **2012**, *51*, 12124; *Angew. Chem.* **2012**, *124*, 12290.
[14] H. Wang, K. Sun, F. Tao, D. J. Stacchiola, Y. H. Hu, *Angew. Chem. Int. Ed.* **2013**, *52*, 9210; *Angew. Chem.* **2013**, *125*, 9380.
[15] J. Wu, M. Agrawal, H. A. Becerril, Z. Bao, Z. Liu, Y. Chen, P. Peumans, *ACS Nano* **2010**, *4*, 43.
[16] T. Sun, Z. L. Wang, Z. J. Shi, G. Z. Ran, W. J. Xu, Z. Y. Wang, Y. Z. Li, L. Dai, G. G. Qin, *Appl. Phys. Lett.* **2010**, *96*, 133301.
[17] H. Meng, J. X. Luo, W. Wang, Z. J. Shi, Q. Niu, L. Dai, G. G. Qin, *Adv. Funct. Mater.* **2013**, *23*, 3324.
[18] J. O. Hwang, J. S. Park, D. S. Choi, J. Y. Kim, S. H. Lee, K. E. Lee, Y.-H. Kim, M. H. Song, S. Yoo, S. O. Kim, *ACS Nano* **2012**, *6*, 159.

[19] N. Li, S. Oida, G. S. Tulevski, S.-J. Han, J. B. Hannon, D. K. Sadana, T.-C. Chen, *Nat. Commun.* **2013**, *4*, 2294.
[20] D. Kim, D. Lee, Y. Lee, D. Y. Jeon, *Adv. Funct. Mater.* **2013**, *23*, 5049 – 5055.
[21] A. Kasry, M. A. Kuroda, G. J. Martyna, G. S. Tulevski, A. A. Bol, *ACS Nano* **2010**, *4*, 3839.
[22] F. Gunes, H.-J. Shin, C. Biswas, G. H. Han, E. S. Kim, S. J. Chae, J.-Y. Choi, Y. H. Lee, *ACS Nano* **2010**, *4*, 4595.
[23] Z. Liu, J. Li, Z.-H. Sun, G. Tai, S.-P. Lau, F. Yan, *ACS Nano* **2012**, *6*, 810.
[24] Y. Kim, J. Ryu, M. Park, E. S. Kim, J. M. Yoo, J. Park, J. H. Kang, B. H. Hong, *ACS Nano* **2014**, *8*, 868.
[25] P. Wei, L. Nan, H. R. Lee, E. Adijanto, L. Ci, B. D. Naab, J. Q. Zhong, J. Park, W. Chen, Y. Cui, Z. Bao, *Nano Lett.* **2013**, *13*, 1890.
[26] P.-H. Ho, Y.-C. Yeh, D.-Y. Wang, S.-S. Li, H.-A. Chen, Y.-H. Chung, C.-C. Lin, W.-H. Wang, C.-W. Chen, *ACS Nano* **2012**, *6*, 6215.
[27] U. N. Maiti, W. J. Lee, J. M. Lee, Y. Oh, J. Y. Kim, J. E. Kim, J. Shim, T. H. Han, S. O. Kim, *Adv. Mater.* **2014**, *26*, 40.
[28] T. Fujinaga, I. Sakamoto, *J. Electroanal. Chem.* **1977**, *85*, 185.
[29] R. D. Howells, J. D. Mc Cown, *Chem. Rev.* **1977**, *77*, 69.
[30] Y.-R. Shin, I.-Y. Jeon, J.-B. Baek, *Carbon* **2012**, *50*, 1465.
[31] S. Tongay, K. Berke, M. Lemaitre, Z. Nasrollahi, D. B. Tanner, A. F. Hebard, B. R. Appleton, *Nanotechnology* **2011**, *22*, 425701.
[32] A. M. Rao, P. C. Eklund, S. Bandow, A. Thess, R. E. Smalley, *Nature* **1997**, *388*, 257.
[33] A. Das, S. Pisana, B. Chakraborty, S. Piscanec, S. K. Saha, U. V. Waghmare, K. S. Novoselov, H. R. Krishnamurthy, A. K. Geim, A. C. Ferrari, A. K. Sood, *Nat. Nanotechnol.* **2008**, *3*, 210.
[34] C. Casiraghi, *Phys. Rev. B* **2009**, *80*, 233407.
[35] a) Y.-J. Choi, S. C. Gong, C.-S. Park, H.-S. Lee, J. G. Jang, H. J. Chang, G. Y. Yeom, H.-H. Park, *ACS Appl. Mater. Interfaces* **2013**, *5*, 3650; b) S.-O. Jeon, H.-S. Lee, Y.-M. Jeon, J.-W. Kim, C.-W. Lee, M.-S. Gong, *Bull. Korean Chem. Soc.* **2009**, *30*, 863; c) H.-Y. Oh, I. Yoo, Y. M. Lee, J. W. Kim, Y. Yi, S. Lee, *Bull. Korean Chem. Soc.* **2014**, *35*, 929.
[36] a) K. Sugiyama, H. Ishii, Y. Ouchi, K. Seki, *J. Appl. Phys.* **2000**, *87*, 295; b) S. Y. Kim, J.-L. Lee, K.-B. Kim, Y.-H. Tak, *J. Appl. Phys.* **2004**, *95*, 2560.

Received: January 14, 2016
Revised: March 7, 2016
Published online: April 13, 2016

